THE EFFECTS OF PANRETINAL PHOTOCOAGULATION ON THE PRIMARY VISUAL CORTEX OF THE ADULT MONKEY*

BY *Joanne A. Matsubara, PhD* (BY INVITATION), *Dawn Y. Lam, BSc* (BY INVITATION), *Ronald E. Kalil, PhD* (BY INVITATION), *B'Ann T. Gabelt, MS* (BY INVITATION), *T. Michael Nork, MD, Dan Hornan, MBBS* (BY INVITATION), AND *Paul L. Kaufman, MD*

ABSTRACT

Purpose: To determine the effects of panretinal photocoagulation (PRP) on the levels of cytochrome oxidase (CO), Zif268, synaptophysin, and growth-associated protein 43 (GAP-43) in the primary visual cortex of adult monkeys.

Methods: Ten adult primates underwent unilateral argon laser PRP with instrument settings at 300 to 500 μm spot diameter, 200 to 500 mW power intensity, and 0.1 to 0.2 second duration, causing moderate to severe burns in the peripheral retina. At 20 hours, 12 days, 6 months, and 13 months after laser treatment, the visual cortex was assessed histologically for CO and immunohistochemically for Zif268, synaptophysin, and GAP-43.

Results: PRP resulted in transneuronal changes in the relative distributions of CO, Zif268, synaptophysin, and GAP-43 in the primary visual cortex. CO activity was relatively decreased in the lasered eye's ocular dominance columns at 12 days post-PRP, with recovery by 13 months post-PRP. The level of Zif268 was dramatically decreased in the lasered eye's ocular dominance columns at 20 hours post-PRP, with gradual recovery by 13 months post-PRP. Levels of synaptophysin and GAP-43 immunoreactivity were increased in both the lasered and the nonlasered eyes' ocular dominance columns at 6 months post-PRP.

Conclusion: PRP treatment results in metabolic activity changes in the visual cortex of the adult monkey. These changes are followed chronologically by spatial redistribution of synaptophysin and GAP-43, neurochemicals known to play a role in cortical plasticity. This study demonstrates, for the first time, that PRP as used in the treatment of diabetic retinopathy results in a redistribution of neurochemicals in the adult monkey visual cortex. Such changes may help explain the anomalous visual functional loss often reported by patients after PRP.

Tr Am Ophth Soc 2001;99:33-43

INTRODUCTION

Diabetic retinopathy is the leading cause of the onset of blindness among adults of working ages (20 to 74 years). Timely treatment with panretinal photocoagulation (PRP) has been found to stop or slow visual loss associated with diabetic retinopathy.[1] Although clinical trials have documented the efficacy of PRP, its mechanism is not clear. One theory proposes that PRP destroys some of the ischemic retina, thereby reducing its production of an angiogenic factor.[2] A second theory suggests that PRP improves oxygenation of the ischemic inner retina by destroying metabolically active photoreceptor cells and allowing diffusion of oxygen from the choriocapillaris to the inner retinal layers.[3-7]

*From the Department of Ophthalmology, University of British Columbia, Vancouver, Canada (Dr Matsubara, Ms Lam, Mr Hornan), and the Center for Neuroscience (Dr Kalil) and Department of Ophthalmology and Visual Science (Dr Kalil, Ms Gabelt, Dr Nork, Dr Kaufman), University of Wisconsin–Madison. Supported by grant EY02698 from the National Eye Institute and grant MT13363 from the Medical Research Council.

Although the exact mechanism underlying the efficacy of PRP is not understood, it is known that photoreceptors in the peripheral retina are destroyed by laser treatment, thus causing partial visual loss in the treated eye.[8] Visual deprivation–by lid suture, intraocular injection of tetrodotoxin (TTX), or enucleation–can cause significant changes in the neurochemistry and organization of the central visual pathways;[9-12] therefore, we were interested in elucidating the central consequences of visual loss associated with PRP. Given the frequency and importance of PRP for diabetic retinopathy, characterizing its effects on the visual cortex, and the consequences to visual function, is worthwhile.

This study focused on the consequences of unilateral PRP on the redistribution of several neurochemicals in the primary visual cortex of the adult monkey. Two metabolic activity markers, cytochrome oxidase (CO) and the immediate early gene product Zif268, were studied because both are down-regulated in response to visual deprivation.[11-14] Zif268 is down-regulated within hours of deprivation,[14] while changes in CO activity usually require days.[11] The effects of PRP on 2 plasticity markers that play

an important role in the formation and maintenance of new synapses in the nervous system, growth-associated protein 43 (GAP-43) and synaptophysin,[15-17] were also evaluated.

METHODS

PHOTOCOAGULATION

Ten adult cynomolgus (*Macaca fascicularis*) and rhesus (*M mulatta*) monkeys were anesthetized with ketamine (10 mg/kg intramuscularly) followed by sodium pentobarbitol (35 mg/kg intramuscularly). The pupils were dilated with 2.5% phenylephrine and 1% tropicamide. The animals were placed prone in a head holder, or held by an assistant, and argon laser light was delivered by a standard slit-lamp system (Coherent model 900 argon laser) through a one-, two- or three-mirror Goldmann-type contact lens, designed and fabricated especially for the monkey eye.[18] Senior retinal specialists T.M. Nork and I.H.L. Wallow performed PRP. One eye of each monkey received argon-green (514 nm) laser burns, analogous to the DRS/ETDRS protocol,[1] with instruments set at a 300 to 500 μm spot diameter, 200 to 500 mW power, and 0.1 to 0.2 second duration. The lasered area extended 20° to 50° from the fovea. Complete PRP consisted of 650 to 1,050 argon lesions and was divided into 2 sessions. Intensity and topography were documented by fundus photography using a Zeiss fundus camera. Details of the PRP given to each animal are in Table I. All experiments were conducted in accordance with the ARVO statement for the use of animals in ophthalmic and vision research.

TISSUE PREPARATION

At the designated post-PRP times (20 hours, 12 days, 6 months, and 13 months), animals were anesthetized with ketamine and surgical-depth sodium pentobarbitol as previously described. The eyes were removed and immersion-fixed in 4% paraformaldehyde in phosphate buffer (PB) or frozen in -80 ºC isopentane. The retina from each immersion-fixed eye was dissected and a whole-mount preparation was photographed to document laser sites.[19] Next, the retina was embedded in O.C.T. and frozen in liquid nitrogen. Cryostat sections of 8-μm thickness were stained with hematoxylin-eosin, and the sites of photocoagulation were assessed for the severity of damage to the neural retina at the light microscopic level (Fig 1).

After enucleation, animals were euthanized and perfused intracardially. Three animals (asterisks, Table I) underwent perfusion with Sorenson's buffer (0.1 M) in 0.9% saline solution. The brains were removed and the occipital lobes divided into blocks representing the fovea (block 1, opercular surface) and the peripheral field (blocks 2, 3, and 4) in the primary visual cortex (area V1) (Fig 2).[20,21] Cortical blocks were flattened between glass slides and frozen in isopentane at -80 °C. Tissue from these 3 animals was used for CO histochemistry and Zif268 immunohistochemistry. The other 7 animals (Table I) were perfused intracardially with PB (0.1 M, pH 7.2) followed by 4% paraformaldehyde in PB. The brains were then removed and stored in cold PB. Brain tissue was blocked and cryoprotected in 20% to 30% sucrose at 4 °C overnight. Tissue from these 7 animals was used for CO histochemistry and immunostaining for Zif268, GAP-43, and synaptophysin.

CYTOCHROME OXIDASE (C)

The cytochrome oxidase histochemical protocol was based on previously documented methods.[22,23] Sections of tissue were incubated for 2 to 4 hours at 40 °C in a solution containing 20 to 25 mg of diaminobenzidine (DAB), 30 mg of cytochrome C, 20 mg of catalase, and 2 g of sucrose dissolved in 100 mL of 0.05 M phosphate buffer (pH, 7.2). The

TABLE I: DETAILS OF PRIMATE PANRETINAL PHOTOCOAGULATION (PRP)

ANIMAL ID	SPECIES	SEX	AGE (YR)	WEIGHT (KG)	SURVIVAL TIME (POST-PRP)	PRP (ARGON GREEN LASER) POWER (MW)	DURATION (SECOND)	SPOT SIZE (μM)	NO. OF BURNS
RQ637*	*Macaca mulatta*	Male	6-8	6.2	20 hr	230-290	0.1	500	1016
AQ60*	*M mulatta*	Male	6-8	5.35	20 hr	250-300	0.2	300	1016
AQ21	*M mulatta*	Male	6-8	5.95	20 hr	250-400	0.2	300	1045
K420	*Macaca fasicularis*	Female	8-10	3.1	12 days	240-280	0.1	500	761
K429	*M fasicularis*	Male	8-10	7.1	12 days	220-260	0.1	500	822
K367	*M fasicularis*	Male	8-10	5.1	12 days	240	0.1	500	877
K374	*M fasicularis*	Male	8-10	5	12 days	240	0.1	500	1021
K415*	*M fasicularis*	Male	8-10	4.1	6 mo	250	0.2	500	660
K414	*M fasicularis*	Male	8-10	4.2	6 mo	220-250	0.2	500	693
K413	*M fasicularis*	Male	8-10	4.9	13 mo	280	0.1	500	706

* Animals that were perfused with Sorenson buffer. All other animals were perfused with 4% paraformaldehyde.

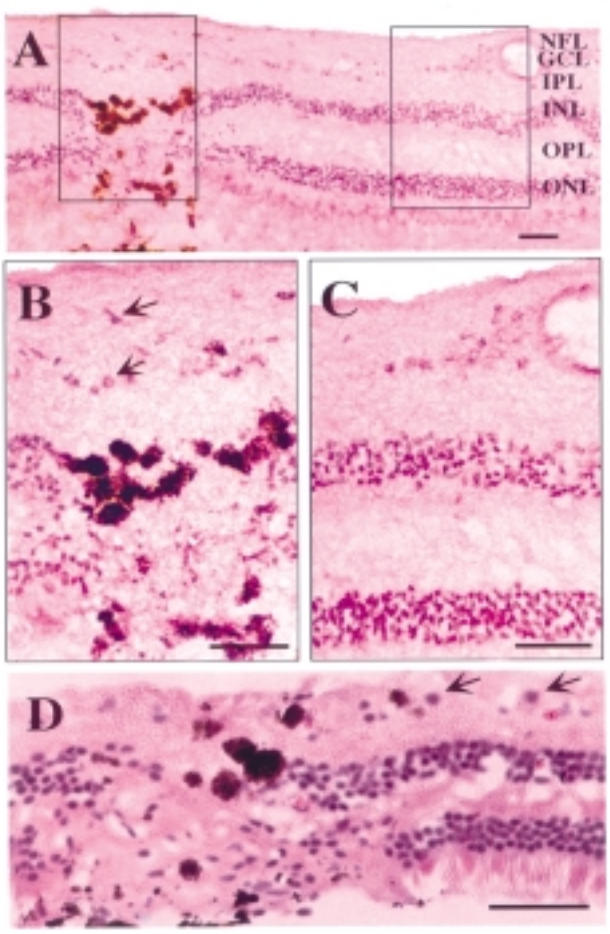

FIGURE 1

Cryostat cross section of retina stained with hematoxylin-eosin at 6 and 13 months post-PRP. A, Predominant damage due to PRP was a grade III burn. Outer retinal layers were severely disrupted with loss of photoreceptor cells. There was moderate disruption to inner nuclear layer with hyperpigmentation (left box). B, Enlargement of left box in A shows a laser site with significant sparing of retinal ganglion cells (arrowheads). C, Enlargement of right box in A shows an interlaser site with intact retinal anatomy. D, At 13 months post-PRP, predominant damage due to PRP was also a grade III burn. Outer retinal layers were severely disrupted with loss of photoreceptor cells. There was moderate disruption to inner nuclear layer with hyperpigmentation. Ganglion cells (arrowheads) were anatomically intact. NFL, nerve fiber layer; GCL, ganglion cell layer; IPL, inner plexiform layer; INL, inner nuclear layer; OPL, outer plexiform layer; ONL, outer nuclear layer. Scale bars =0.1 mm.

reaction was intensified by the addition of 1% nickel ammonium sulfate (3 to 5 mL) and 1% cobalt chloride (3 to 5 mL).

ZIF268, GAP-43, AND SYNAPTOPHYSIN IMMUNOHISTOCHEMISTRY

Monoclonal antibodies against the phosphorylated and nonphosphorylated forms of GAP-43 and the 38 kDa band of synaptophysin were obtained from Sigma-Aldrich Co (St Louis, Mo). The polyclonal antibody against Zif268 was obtained from Dr R. Bravo. All cortical blocks were

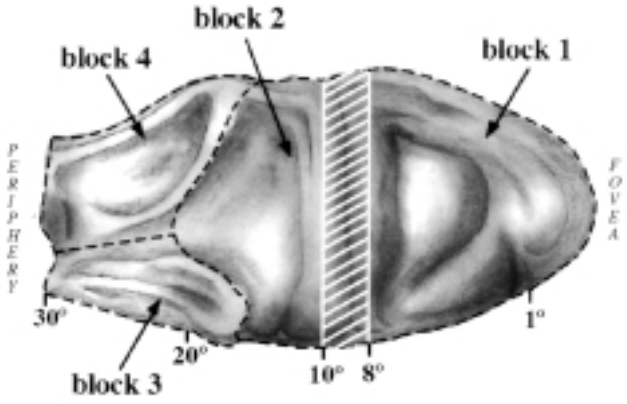

FIGURE 2

Schematic view of macaque's entire primary visual cortex from a flattened preparation,[20,21] identifying the boundaries of tissue blocks processed in this study. Block 1 is dorsal opercular surface, representing approximately the central 10º of visual field. Block 2 is roof of the calcarine sulcus, representing approximately 10º to 30º eccentricity. Hatched area between blocks 1 and 2 is the "hinge," where operculum folds into the calcarine sulcus, which in our preparation was not accessible. Blocks 3 and 4 are ventral and dorsal banks of the calcarine stem, respectively. Blocks 3 and 4 include peripheral visual field representation, approximately 15º to 60º eccentricity.[21]

frozen and cut at 50 μm tangential to the pial surface. Tissue sections were placed in a solution containing rabbit polyclonal antisera selective for Zif268, at a 1:10,000 dilution in PB with 3% normal goat serum, for at least 48 hours at 4°C.[13] The sections were then washed in PB containing 0.3% Triton X-100 and incubated for 2 hours at room temperature in a 1:1,000 dilution of biotinylated goat anti-rabbit secondary antibody in 0.3% Triton X-100 in PB. After washing with PB, the sections were incubated for 1 hour at room temperature in a solution of avidin-biotin conjugated horseradish peroxidase complex (Vector Labs, Burlington, Calif). Sections were then subjected to a nickel-enhanced DAB reaction.

Synaptophysin and GAP-43 immunohistochemistry was performed using a 1:1,000 dilution of antisera in PB with 0.1% Triton X-100 and 3% normal horse serum. Sections were incubated for 48 hours at 4°C, then washed 3 times with 0.3% Triton X-100 in PB and placed into a solution containing biotinylated horse anti-mouse secondary antibody at a dilution of 1:1,000 in 0.3% Triton X-100 and 3% normal horse serum in PB. Bound antibody was then visualized with the glucose oxidase-DAB reaction. All sections were mounted onto gelatinized slides, air-dried, and coverslipped. The primary antibody was absent in control sections, which were otherwise processed identically.

DATA ANALYSIS

Layer 4C

Video images of tissue sections processed for CO, Zif268, synaptophysin, and GAP-43 were captured with a COHU

CCD (4915) camera using a Macintosh IIfx-based analysis system with a Data Translation DT-2255 quick capture board. NIH Image 1.62 was used to obtain density profiles and to measure periodicity of ocular dominance columns. Optical density was measured in lasered and nonlasered eye ocular dominance domains. Because CO-stained tissues demonstrated a uniform staining pattern at 20 hours post-PRP, we identified ocular dominance columns by Zif268 immunoreactivity. For the other post-PRP time points, CO histochemistry was used to identify the lasered (light bands) and nonlasered (dark bands) eye columns. To demonstrate that the light and dark bands in synaptophysin and GAP-43 immunoreacted tissue coincided with lasered or nonlasered eye ocular dominance columns, tissue sections were co-aligned with alternate serial sections processed for CO or Zif268. For the 4 neurochemicals and at each post-PRP time point, 10 transects were taken in the lightly stained eye bands and also in the adjacent darkly stained bands. Density ratios between neighboring bands were calculated as the fraction of lasered over nonlasered eye band densities. Mean density ratio was calculated from 10 density ratios.

Estimates of baseline levels of synaptophysin and GAP 43 were obtained from densiometric measures of immunostaining in visual cortical block 1, the foveal representation, which appeared unaffected by PRP treatment (Table II).

Statistics were performed on density ratios using the *t* test and the analysis of variance (ANOVA) test. Lasered eye–nonlasered eye density ratios of 1, <1, or >1 were possible. Ratios of 1 represented uniform staining between adjacent ocular dominance bands. Ratios of <1 indicated that the lasered eye columns were less intensely stained than the adjacent, nonlasered eye columns, and the opposite was true for ratios of >1. A two-tailed *t* test compared the density ratio at each time point to the uniform staining intensity ratio of 1. The *P* value for the null hypothesis was set below 0.01. For each neurochemical marker, differences between mean density ratios for the 4 time points were evaluated by the ANOVA statistical test.

TABLE II: PERCENTAGE OF CORTICAL TISSUE EXHIBITING OCULAR DOMINANCE BANDS (ODB)

ANIMAL ID	SURVIVAL TIME	BLOCK NO	AREA WITH ODB (MM^2)	TOTAL AREA (MM^2)	% AREA WITH ODB
K429R	12 days	1	0	262.6	0
	(CO*)	2	92.6	121.4	76.3
		3	50.2	119.7	42.0
		4	129.7	188.4	68.8
K420R	12 days	1	0	152.6	0
	(CO)	2	51.5	69.1	74.5
		3	10.1	83.7	12.1
		4	106.5	139.8	76.1
K367R	12 days	1	0	377.9	0
	(CO)	2	87.8	170.4	51.5
		3	13.6	190.9	7.1
		4	42.5	343.4	12.4
K414R	6 months	1	0	216	0
	(CO)	2	66.7	101.9	65.4
		3	61.5	152.4	40.4
		4	194.8	265.5	73.4

*CO, cytochrome oxidase.

Layer 2/3

In layer 2/3 CO blobs were captured and blob density was measured with the same video system and image program previously described. Optical density of neighboring CO blob rows was again compared as the fraction of lasered over nonlasered eye blob densities. Statistical analysis, as previously described, was used to compare blob density ratios to the uniform staining intensity ratio. In addition, ten transects that ran perpendicular to ocular dominance columns were used to measure blob periodicity.

RESULTS

RETINAL HISTOLOGY

The spot diameter, duration, power, and number of laser burns per case are given in Table I. The mean distance between laser sites was calculated to be 1.5 spot diameters (750 μm). It is estimated that about 20% of the retina was lasered during PRP. Figure 1 illustrates 8-μm cryostat sections of the retina stained with hematoxylin-eosin at 6 months (Fig 1 A through C, case K414) and at 13 months (Fig 1D, case K413) post-PRP. Histopathological analysis revealed that the predominant damage to the retina from PRP was a mild to moderate grade III burn.[8] The lasered sites were characterized by hyperpigmentation and disruption of the retina, especially the inner nuclear layer, the outer plexiform layer, and the outer nuclear layer. The retinal ganglion cell layer was histologically intact (arrows, Figs 1B, 1D). The interlaser sites demonstrated normal retinal histology (Fig 1C).

CO STAINING IN LAYER 4C OF THE VISUAL CORTEX

20 Hours Post-PRP

CO staining appeared uniform throughout layer 4C at 20 hours post-PRP (Fig 3E). The optical density values of CO staining in lasered and nonlasered ocular dominance columns confirmed our qualitative observation that CO density was statistically similar in adjacent eye bands at 20 hours post-PRP (Fig 4A).

12 Days and 6 Months Post-PRP

Stripe-like fluctuations in CO histochemistry of layer 4C were observed at 12 days and 6 months post-PRP

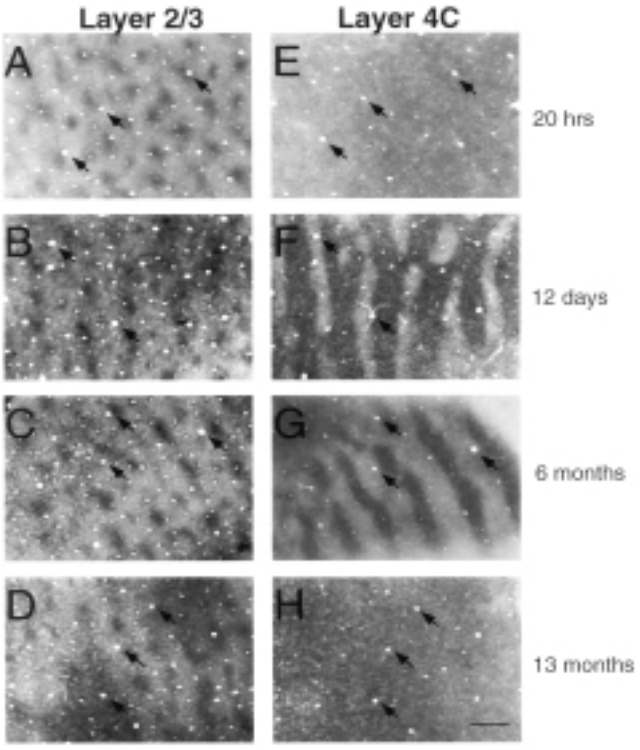

FIGURE 3

Cytochrome c oxidase–stained tangential sections through layers 2/3 and 4C at 20 hours, 12 days, 6 months, and 13 months post-PRP. A and E, 20 hours post-PRP. No visible effects of deprivation on CO staining of blobs (A) or in thalamic recipient zone in layer 4C (E). Mean density ratio (lasered/normal eye) of 0.993 ± 0.002 SEM in layer 4C was not significantly different from a normal density ratio of uniform staining. B and F, 12 days post-PRP. Rows of shrunken blobs (B) were located overlying pale ocular dominance bands of layer 4C (F). Mean density ratio of CO blobs at 12 days post-PRP was 0.70 ± 0.11, significantly <1. Ocular dominance bands were visible in layer 4C of blocks 2, 3, and 4 but not in block 1. Mean density ratio in layer 4C for 12 days post-PRP was 0.89 ± 0.02, significantly <1. C and G, 6 months post-PRP. Shrunken rows of CO blobs (C) align with light ocular dominance bands (G). Mean density ratio in layer 4C for 6 months post-PRP was 0.69 ± 0.04, significantly <1. D and H, Density of neighboring rows of CO blobs at 13 months post-PRP was equivalent (D). At 13 months post-PRP, stripe-like fluctuations in CO staining between lasered and nonlasered eyes' ocular dominance bands in layer 4C were no longer present (H). In layer 4C, mean density ratio of 0.98 ± 0.09 was not significantly different from a uniform density ratio of 1. Scale bar = 1 mm.

(Figs 3F, 3G). These fluctuations presumably represent ocular dominance columns, with the lightly stained CO area representing the lasered eye's cortical columns and the darkly stained CO area representing the nonlasered eye's cortical columns.[11] The fluctuating pattern of CO staining was only observed in cortical areas representing the peripheral visual fields (Table II, data for blocks 2, 3, and 4). Cortical areas representing central vision (Table II, data for block 1) exhibited uniform staining in layer 4C.

As the retina is topographically represented in visual cortex, metabolic activity changes caused by unilateral PRP deprivation should also demonstrate topographic

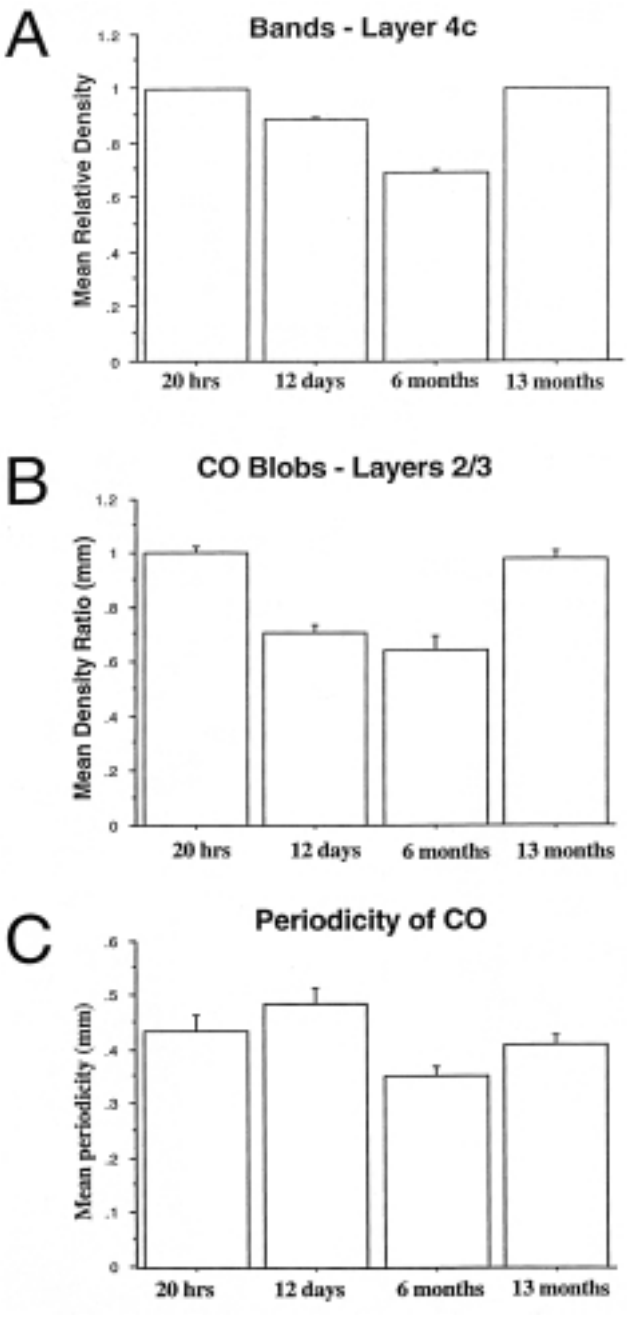

FIGURE 4

Summary graphs identifying time course of changes in density and periodicity levels of CO after PRP treatment. Data are mean density ratios (lasered eye/normal eye) ± SEM. A, Gradual reduction in CO activity in lasered eye's ocular domains bands at 20 hours (1.00 ± .01), 12 days (.886 ± .025), and 6 months post-PRP (.693 ± .041), with recovery to baseline levels by 13 months post-PRP (1.00 ± .01). Effects of PRP on optical density and periodicity of CO blobs in layer 2/3 (B). Mean density ratios (lasered eye/normal eye) of CO blobs in layer 2/3. At 12 days and 6 months post-PRP, density of CO blobs was significantly <1 ($P < .01$). At 20 hours and 13 months post-PRP, density of CO blobs was not significant. C, Mean periodicity of CO blobs in layer 2/3 ranged from 0.35 to 0.48 mm.

registry. We calculated the area of visual cortex that exhibited light and dark CO columns at 12 days and 6 months post-PRP (Table II) to be greater than 50% of the lower peripheral visual fields (blocks 2, 4). In contrast, less than 50% of the upper peripheral visual field (block 3) exhibited CO fluctuations.

13 Months Post-PRP

No discernible fluctuation in CO staining was observed in layer 4C at 13 months post-PRP (Fig 3H). Figure 4A illustrates the time course of changes in CO density in layer 4C.

CO STAINING IN LAYER 2/3

CO blobs at 20 hours post-PRP appeared uniform (Figs 3A and 5A). Note that in Fig 5B the density of neighboring rows of CO blobs at 20 hours is equivalent. At 12 days (Fig 3B) and 6 months post-PRP (Fig 3C), CO blobs centered over the lasered eye bands were both paler and smaller, compared with blobs centered over the nonlasered eye bands. Examples of transects used for measuring optical density and periodicity of CO blobs at 6 months post-PRP are shown in Figs 5C and 5D. By 13 months post-PRP, the density of neighboring rows of CO blobs was equivalent again (Fig 3D).

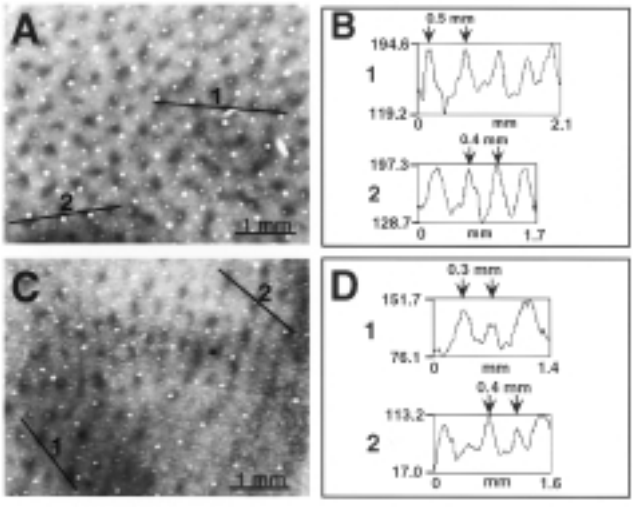

FIGURE 5

Density and periodicity of CO blobs in layer 2/3. Transects through several neighboring rows of CO blobs drawn perpendicular to ocular dominance band orientation as demonstrated by anti-Zif268 immunoreactivity for 20 hours post-PRP (A) or by CO histochemistry for 6 months post-PRP (C). Density values along transects (B, D). Arrows indicate an example of two neighboring blobs from each transect; value between arrows represents distance between blobs. A and B, 20 hours post-PRP. CO blobs of neighboring rows demonstrated uniform density, with a mean density ratio of 1.00 ± 0.08. Mean periodicity was 0.44 ± 0.10 mm. C and D, 6 months post-PRP. CO blobs displayed nonuniform density; rows of pale CO blobs alternated with rows of dark CO blobs. Mean density ratio for 6 months post-PRP was 0.65 ± 0.16. Both values were significantly <1 (P< .01). Mean periodicity was 0.35 ± 0.07 mm for 6 months post-PRP.

ZIF268 IMMUNOHISTOCHEMISTRY

Figure 6 illustrates immunostaining for Zif268 in layer 4C at 4 time points post-PRP. Darkly immunoreactive nuclei, seen as punctate staining, form a banded pattern (asterisks, Figs 6A, 6B, 6C). Figure 6A demonstrates bands of reduced immunostaining, representing the lasered eye, interdigitated with bands of dark immunostaining (asterisks) from the nonlasered eye at 20 hours post-PRP. At 12 days post-PRP, Zif268 immunohistochemistry again revealed a fluctuating pattern of lightly and darkly immunostained bands, though the contrast was less distinct than at 20 hours post-PRP (Fig 6B). At 6 months post-PRP, the difference between light and dark bands was just visible (Fig 6C), and by 13 months post-PRP there were no detectable bands present (Fig 6D).

SYNAPTOPHYSIN IMMUNOHISTOCHEMISTRY

Synaptophysin immunohistochemistry resulted in uniform staining in all cortical layers except layer 4C. Figure 7 illustrates results from layer 4C at 4 time points post-PRP. Bands in layer 4C stained for synaptophysin were observed only at 6 months post-PRP (Fig 7G). Comparisons with CO tissue (Fig 7C) revealed that the darkly stained synaptophysin bands (Fig 7F) coaligned with darkly stained CO bands, representing the nonlasered eye columns. While a relative difference in density was visible (Fig 7G), the density of both the lasered and the nonlasered eyes' columns was greater than that of visual cortex from block 1, which represented baseline levels of synaptophysin in this study. The area that demonstrated synaptophysin bands was calculated to be 35 mm^2, or approximately 13% of the cortical area that demonstrated a deprivation effect (loss of CO activity associated with the lasered eye).

GAP-43 IMMUNOHISTOCHEMISTRY

Immunostaining using an antibody against GAP-43 also demonstrated a similar laminar pattern of labeling and time course as synaptophysin. Figure 8 shows serial sections stained for Zif268 (Fig 8A), CO (Fig 8B, C, D), and GAP-43 (Fig 8E, 8F, 8G, 8H). We observed uniform GAP-43 immunostaining at 20 hours, 12 days, and 13 months post-PRP (Fig 8E, 8F, 8H). However, GAP-43 bands were seen at 6 months post-PRP (Fig 8G). Comparisons with CO tissue (Fig 8C) revealed that the darkly stained GAP-43 bands aligned with the darkly stained CO bands associated with the nonlasered eye. As seen for synaptophysin immunoreactivity, density levels in the lasered and nonlasered eye columns were both higher than seen in the visual cortex of block 1, representing the

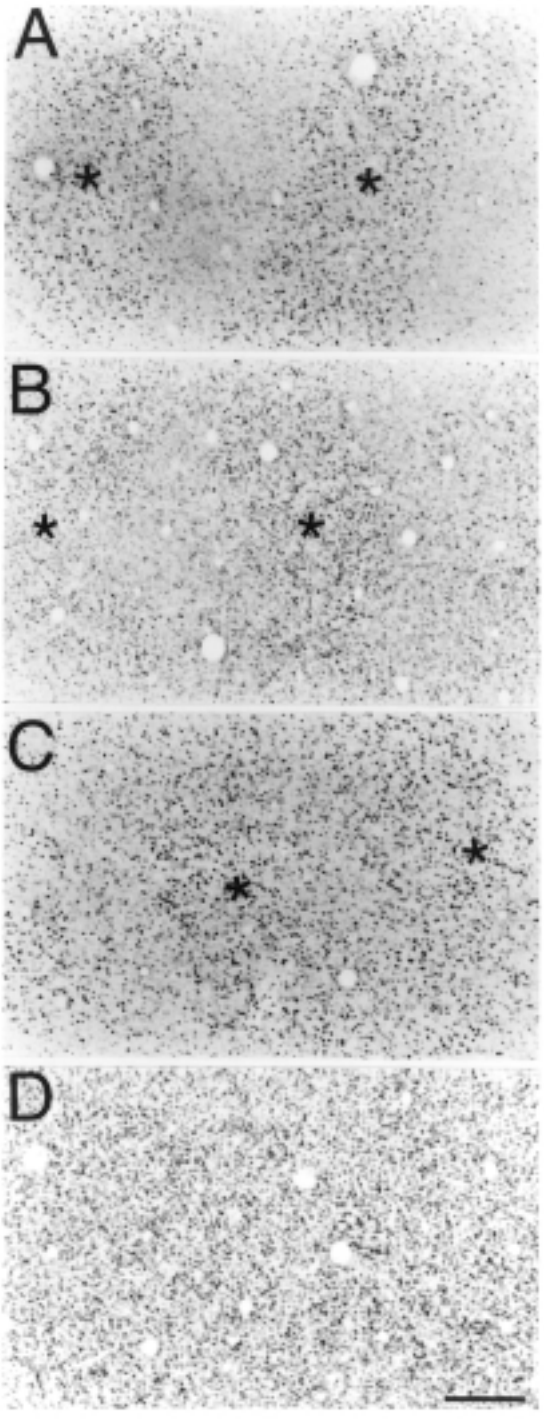

FIGURE 6

Comparisons of Zif268 immunoreactivity at 4 time points post-PRP. A, Anti-Zif268 immunostaining in layer 4C at 20 hours post-PRP demonstrates series of dark immunoreactive bands (asterisks), which represent ocular dominance bands of nonlasered eye, separated by light immunoreactive bands, which represent ocular dominance bands of lasered eye. B, Dark immunoreactive bands associated with nonlasered eye (asterisks) are still evident 12 days post-PRP. C, By 6 months post-PRP, contrast between dark and light bands is considerably less as immunostaining levels increase in lasered eye bands compared with nonlasered eye bands (asterisks). D, at 13 months post-PRP, unifom Zif268 immunoreactivity is present. Scale bar = 200 µm.

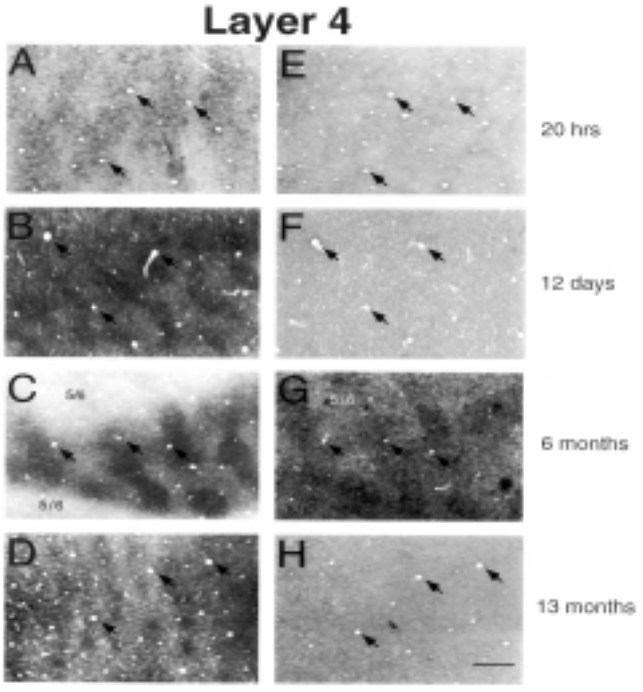

FIGURE 7

Comparisons of ocular dominance bands and synaptophysin immunoreactivity at 4 time points post-PRP. A, Anti-Zif268 immunostaining in layer 4C at 20 hours post-PRP. B and C, At 12 days and 6 months post-PRP, CO bands were evident through layer 4C. D, Rows of CO blobs in layer 2/3 identify orientation of ocular dominance bands at 13 months post-PRP. E, F, G, and H, Synaptophysin immunohistochemistry. At 20 hours (E), 12 days (F), and 13 months (H) post-PRP, there was no differential immunolabeling for synaptophysin between lasered and nonlasered eye columns. At 6 months post-PRP (G), a series of darkly staining synaptophysin immunoreactive bands was present in layer 4C. Mean density ratio of synaptophysin immunostaining at 6 months post-PRP (0.98 ± 0.01) was significantly different from a uniform density ratio of 1 ($P < .01$) (Fig 8G). Alignment with sections stained for CO revealed that strongly immunoreactive bands co-localized with normal eye bands. Arrows identify cross sections of radially penetrating blood vessels used for alignment of serial sections. Scale bar =1 mm.

fovea and thus unimpaired by PRP. The area that demonstrated GAP-43 bands was calculated to be 35 mm^2, approximately 12% of the cortical area that demonstrated deprivation effect (loss of CO activity associated with the lasered eye).

DISCUSSION

Previous studies have looked at the cortical changes arising after single central retinal laser lesions in the cat [24-26] and the primate.[10] This is the first study to look at the effects of multiple laser sites in the peripheral retina, as used in PRP therapy. This study focused on visual cortical changes in metabolic activity markers (CO and Zif268) and cortical plasticity markers (synaptophysin and GAP-43). We found that the levels changed in response to partial deafferentation by unilateral PRP. Of particular

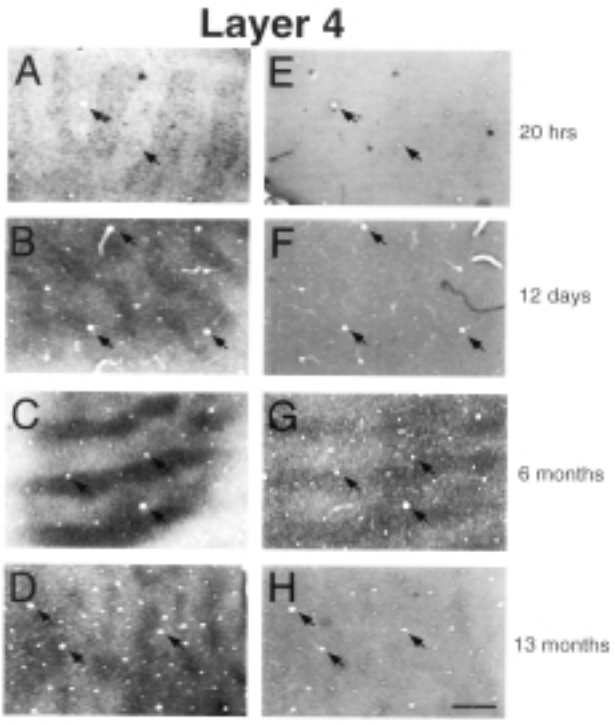

FIGURE 8
Comparisons of ocular dominance bands and GAP-43 immunoreactivity at 4 time points post-PRP. A, At 20 hours post-PRP, Zif268 immunostaining revealed a series of ocular dominance bands. At 12 days (B) and 6 months (C) post-PRP, CO histochemistry revealed ocular dominance bands in layer 4C. D, At 13 months post-PRP, rows of CO blobs in layer 2/3 identify direction of elongation of ocular dominance domains. At 20 hours (E), 12 days (F), and 13 months (H) post-PRP, uniform immunostaining for GAP 43 was observed across both lasered and normal eye ocular dominance domains. At 6 months post-PRP (G), a series of darkly staining GAP-43 immunoreactive bands was present in layer 4C of block 4, and mean density ratio of 0.98 ± 0.01 was significant <1 ($P < .01$). Alignment with sections stained for CO revealed that strongly immunoreactive bands co-localized with normal ocular dominance bands. Arrows identify cross sections of radially penetrating blood vessels used for alignment of serial sections. Scale bar =1 mm.

interest is the finding that synaptophysin and GAP-43 levels are greater in both the lasered and nonlasered eyes' ocular dominance columns at 6 months post-PRP, compared with baseline levels found in nondeprived visual cortex.

CO ACTIVITY

We found no change in CO activity at 20 hours post-PRP, in contrast with the study of Wong-Riley and associates,[12] which reported a reduction in CO activity as early as 14 hours after an intraocular TTX injection. It is likely that intraocular TTX injection silences all ganglion cells, whereas PRP may silence only ganglion cells within the laser sites, estimated at 20% of the retina. The difference in results is probably due to the more severe form of deprivation used in the study of Wong-Riley and associates. At 12 days and 6 months post-PRP, a gradual reduction in CO staining in the lasered eye's ocular dominance columns (layer 4C) and in the overlying CO blobs (layer 2/3) was seen (Fig 4A, 4B). By 13 months post-PRP, the CO activity associated with the lasered eye's ocular dominance columns returned to levels equaling those of the nonlasered eye's ocular dominance columns (Fig 4A). The recovery of CO activity by 13 months post-PRP likely indicates a recovery of retinal ganglion cell metabolism, as our analysis revealed anatomically intact ganglion cells within the laser sites of the 13-month post-PRP eye (Fig 1D).

The reduction in CO activity in layer 4C of the 12-day and 6-month post-PRP cases covered the cortical representation of both laser and interlaser sites, as evidenced by the ocular dominance bands. Intuitively, this was surprising and suggests that laser photocoagulation may affect a visual field larger than that represented in the laser sites. Given that the histologic sections of the lasered retina showed that the interlaser sites were anatomically normal (Fig 1A, 1B), we can only speculate that the finding of reduced CO activity in the cortical representation of the interlaser sites is due to central mechanisms, consistent with Wong-Riley's earlier finding from the transition zone of a single focal laser lesion of retina.[12] Alternatively, reduced CO activity in the cortical representation of the interlaser sites may be due to a peripheral mechanism. It would be important to know whether the interlaser sites are visually responsive after PRP treatment. We do not know of any study that has attempted microperimetry of interlaser sites in patients post-PRP.

ZIF268

Zif268 is one of a family of immediate early gene products that were shown to be expressed in neurons in an activity-dependent manner.[27,28] In this study, it was used to identify ocular dominance bands at 20 hours post-PRP, a time point that did not demonstrate effects on CO activity. An earlier study from our laboratory[13] demonstrated that Zif268 immunoreactivity still delineates ocular dominance bands in the primate visual cortex after a 3-month unilateral enucleation. The resultant blurring of ocular dominance bands seen in the present study at 6 months and 13 months post-PRP is consistent with and extends our earlier findings[13] demonstrating that Zif268 levels recover to nondeprived levels between 6 and 13 months post-PRP. Whether this time frame of recovery holds for more severe forms of deprivation, such as enucleation or optic nerve transection, is not known.

CORTICAL PLASTICITY MARKERS

Synaptophysin is a presynaptic 38 kDa vesicle membrane glycoprotein[29] that is expressed during development and in parallel with the formation of new synapses.[29-31] GAP-43 is

expressed at high levels and transported to growth cones and immature synapses during neuronal development[32,33] and has been implicated in axonal growth, synaptic plasticity, and neuronal remodeling.[34,35] There is evidence that GAP-43 can be up-regulated in adult visual cortex after infusion of nerve growth factor in vivo.[36] In the present study, immunohistochemical localization of synaptophysin and GAP-43 at 6 months post-PRP revealed that the nonlasered eye bands were significantly darker than the lasered eye bands (Fig 8D). Further analysis revealed that the levels of synaptophysin and GAP-43 in both lasered and nonlasered bands were significantly higher than levels found in cortex representing the fovea, which is not targeted by PRP. These results suggest that there is an up-regulation of synaptophysin and GAP-43 within layer 4C of both the lasered and nonlasered eyes' ocular dominance columns at 6 months post-PRP.

CLINICAL RELEVANCE

A previous study[37] examined the aspects of visual function necessary in the everyday lives of diabetic patients and identified that tasks involving depth perception, judging distances, navigating stairs, and participating in sports were commonly cited as becoming more difficult since PRP treatment. The current clinical practice is to give PRP unilaterally in any given session. In patients who require bilateral PRP, the second eye is treated after a variable delay of 2 weeks to 2 months. Since our results show that unilateral PRP affects the levels of neurochemicals in the cortical representation of both lasered and nonlasered eyes, imbalances due to synaptic remodeling between eye domains may result in loss of peripheral visual function after PRP treatment. If this is indeed the case, it might be helpful, for those patients requiring bilateral treatment, to separate the PRP sessions between eyes by a week or less. Of course, clinical studies would have to be done to determine if changing the current PRP strategy might improve the quality of life for patients with proliferative diabetic retinopathy.

ACKNOWLEDGEMENTS

The authors thank Ms Eleanor To for expert technical and graphic assistance; Ingolf H. L. Wallow, MD, for performing some PRP treatments; David Grosof, Qiang Gu, Christian Wong, and Tara Stewart for helpful comments on the manuscript; and Jing Cui for preparing and analyzing the histologic slides of the retina. Dr Rodrigo Bravo kindly provided the antibody against Zif268.

REFERENCES

1. Diabetic Retinopathy Study Research Group. Diabetic retinopathy study: Report 6. Design, methods, and baseline results. *Invest Ophthalmol Vis Sci* 1981;21:149-209.
2. Frank N. Etiologic mechanisms in diabetic retinopathy. In: Ryan SJ, ed. *Retina*. Vol 2. St Louis: Mosby; 1989;301-326.
3. Landers MB III, Stefansson E, Wolbarsht ML. Panretinal photocoagulation and retinal oxygenation. *Retina* 1982;2:167-175.
4. Stefansson E, Landers MB III, Wolbarsht ML. Increased retinal oxygen supply following pan-retinal photocoagulation and vitrectomy and lensectomy. *Trans Am Ophthalmol Soc* 1981;79:307-334.
5. Stefansson E, Landers MB III, Wolbarsht ML. Oxygenation and vasodilatation in relation to diabetic and other proliferative retinopathies. (Review) *Ophthalmic Surg* 1983;14:209-226.
6. Wolbarscht ML, Landers MB III, Stefansson E. Vasodilation and the etiology of diabetic retinopathy: A new model. *Ophthalmic Surg* 1981;12:104-107.
7. Wolbarscht ML, Landers MB III. The rationale of photocoagulation therapy for proliferative diabetic retinopathy: A review and a model. (Review) *Ophthalmic Surg* 1980;11:235-245.
8. Wallow I. Clinicopathologic correlation of retinal photocoagulation in the human eye. In: Wengeist TA, Sneed SR, eds. *Laser Surgery in Ophthalmology: Practical Applications*. Norwalk, Conn: Appleton & Lange; 1992;15-27.
9. Hendry SHC, Jones EG. Reduction in number of immunostained GABAergic neurons in deprived-eye dominance columns of monkey area 17. *Nature* 1986;320:750-753.
10. Horton JC, Hocking DR. Monocular core zones and binocular border strips in primate striate cortex revealed by the contrasting effects of enucleation, eyelid suture, and retinal laser lesions on cytochrome oxidase activity. *J Neurosci* 1998;18:5433-5455.
11. Wong-Riley M, Carroll EW. The effect of impulse blockage on cytochrome oxidase activity in the monkey visual system. *Nature* 1984;307:262-264.
12. Wong-Riley M. Primate visual cortex: Dynamic metabolic organization and plasticity revealed by cytochrome oxidase. In: Peters A, Rockland KS, eds. *Cerebral Cortex, Primary Visual Cortex in Primates*. Vol 10. New York: Plenum Press; 1994;141-200.
13. Chaudhuri A, Matsubara JA, Cynader MS. Neuronal activity in primate visual cortex assessed by immunostaining for the transcription factor Zif268. *Vis Neurosci* 1995;12:35-50.
14. Herdegen T, Leah JD, Zimmermann M, et al. The KROX-24 protein, a new transcription regulating factor: Expression in the rat central nervous system following afferent somatosensory stimulation. *Neurosci Lett* 1990;120:21-24.
15. Wong-Riley M, Carroll EW. Effect of impulse blockage on cytochrome oxidase activity in monkey visual system. *Nature* 1984;307:262-264.
16. Benowitz LI, Routtenberg A. A membrane phosphoprotein associated with neural development, axonal regeneration, phospholipid metabolism, and synaptic plasticity. *Trends Neurosci* 1987;10:527-532.
17. Devoto SH, Barnstable CJ. SVP38: A synaptic vesicle protein whose appearance correlates closely with synaptogenesis in the rat nervous system. *Ann NY Acad Sci* 1987;493:493-496.
18. Kaufman PL, Wallow IH. Minified diagnostic contact lenses for biomicroscopic examination and photocoagulation of the anterior and posterior segment in small primates. *Exp Eye Res* 1985;40:883-885.
19. Stone J. Preparation of whole mounts. In: *The Wholemount Book: A Guide to the Preparation and Analysis of Retinal Wholemounts*. Sidney, Australia: Maitland Publications; 1981;2-65
20. Horton JC, Hocking DR. Intrinsic variability of ocular dominance column periodicity in normal macaque monkeys. *J Neurosci* 1996;16:7228-7239.
21. Van Essen DC, Newsome WT, Maunsell JHR. The visual field representation in striate cortex of the macaque monkey: Asymmetries and anisotropies, and individual variability. *Vis Res* 1984;24:429-448.
22. Boyd JD, Matsubara JA. Laminar and columnar patterns of geniculocortical projections in the cat: Relationship to cytochrome oxidase. *J Comp Neurol* 1996;365:659-682.

23. Crockett DP, Maslany S, Harris SL, et al. Enhanced cytochrome-oxidase staining of the cuneate nucleus in the rat reveals a modifiable somatotopic map. *Brain Res* 1993;612:41-55.
24. Baekelandt V, Arckens L, Annaert W, et al. Alterations in GAP-43 and synapsin immunoreactivity provide evidence for synaptic reorganization in adult cat dorsal lateral geniculate nucleus following retinal lesions. *Eur J Neurosci* 1994;6:754-765.
25. Baekelandt V, Eysel UT, Orban GA, et al. Long-term effects of retinal lesions on growth-associated protein 43 (GAP-43) expression in the visual system of adult cats. *Neurosci Lett* 1996;208:113-116.
26. Schmid LM, Rosa M, Calford M, et al. Visuotopic reorganization in the primary visual cortex of adult cats following monocular and binocular retinal lesions. *Cerebral Cortex* 1996;6:388-405.
27. Sagar SM, Sharp FR, Curran T. Expression of c-fos protein in brain: Metabolic mapping at the cellular level. *Science* 1988;240:1328-1331.
28. Dragunow M, Faull R. The use of c-fos as a metabolic marker in neuronal pathway tracing. (Review) *J Neurosci Methods* 1989;29(3):261-265.
29. Wiedenmann B, Franke WW. Identification and localization of synaptophysin, an integral membrane glycoprotein of Mr 38,000 characteristic of presynaptic vesicles. *Cell* 1985;41:1017-1028.
30. Knaus P, Betz H, Rehm H. Expression of synaptophysin during postnatal development of the mouse brain. *J Neurochem* 1986;47:1302-1304.
31. Voigt T, De Lima AD, Beckmann M. Synaptophysin immunohistochemistry reveals inside out pattern of early synpatogenesis in ferret cerebral cortex. *J Comp Neurol* 1993;330:48-64.
32. McIntosh H, Daw N, Parkinson D. Gap-43 in the cat visual cortex during postnatal development. *Vis Neurosci* 1990;4:585-593.
33. Meiri KF, Pfenninger KH, Willard MB. Growth-associated protein, GAP-43, a polypeptide that is induced when neurons extend axons, is a component of growth cones and corresponds to pp46, a major polypeptide of a subcellular fraction enriched in growth cones. *Proc Natl Acad Sci USA* 1986;83:3537-3541.
34. Lovinger DM, Akers RF, Nelson RB, et al. A selective increase in phosphorylation of protein F1, a protein kinase C substrate, directly related to 3 day growth of long term synaptic enhancement. *Brain Res* 1985;343:137-143.
35. Nelson RB, Routtenberg A. Characterization of protein F1 (47 kDa, 4.5 pI): Kinase C substrate directly related to neural plasticity. *Exp Neurol* 1985;89:213-224.
36. Liu Y, Meiri KF, Cynader MS, et al. Nerve growth factor induced modification of presynaptic elements in adult visual cortex in vivo. *Brain Res* 1996;732:36-42.
37. Russell PW, Sekuler R, Fetkenhour C. Visual function after panretinal photocoagulation: A survey. *Diabetes Care* 8(1):57-63.

DISCUSSION

DR LEONARD M. PARVER. The authors have presented experimental results showing the consequences of PRP on the visual cortex. They investigated the effects of unilateral PRP on the distribution of several neurochemical markers in the primary visual cortex of the monkey eye at multiple time periods.

The results of their experiments demonstrate changes in the visual cortex following unilateral PRP. A number of their observations deserve further comment. To begin, their finding that the ocular dominance columns representing both the lasered and non-lasered eye show changes in synaptophysin and GAP-43 levels following unilateral PRP is left unexplained. Further, the authors noted asymmetrical changes in the topographic representations in the visual cortex for the lower and upper visual fields even though presumably they received similar amounts of photocoagulation. The latter finding may be a consequence of sampling given the limited number of animals examined at any one point in time.

The authors also noted changes in the visual cortex representation for both lasered and interlasered sites. They speculate that the extent of the field changes seen at the visual cortex level is somehow greater than the site occupied by the laser burn. An alternate explanation is that the area of retina damaged during PRP is greater than the area represented by the visible retinal scars and represents the effects of indirect photochemical injury. Indirect photochemical damage to the macula of the monkey eye following PRP has been reported.[1] The changes observed were not visible on ophthalmoscopy or fluorescein angiography but were present on EM and confined to the RPE and outer photoreceptor layers. The authors examined the retina using only light microscopy. If there was evidence of photochemical injury, it may have been detectable only by EM. The authors did examine the region of the visual cortex representing the fovea and noted no changes using their neurochemical markers. One wonders whether this represents a threshold effect and whether the neurochemical markers require a certain level of damage to trigger changes in the topographic representation in the visual cortex.

The DRS and the ETDRS established the efficacy of PRP in the treatment of proliferative diabetic retinopathy. Subsequent clinical experience has proven these conclusions to be correct. As with any treatment, however, there are potential unwanted side effects. In the case of PRP, there was an unexplained loss in Snellen visual acuity first observed in the DRS and later confirmed in the ETDRS. Between 3% and 11% of patients suffer a loss of Snellen vision of 1 to 2 lines. Even in patients who do not demonstrate a loss of Snellen visual acuity, other more sensitive tests of visual function, such as contrast sensitivity, have uncovered visual abnormalities. The authors have proposed that their findings in the visual cortex following PRP may help explain this observed loss of Snellen visual acuity. While their findings could potentially support changes in peripheral vision following PRP, it is difficult to understand how changes solely in the topographic representation of peripheral retinal regions could effect central or macular visual tasks such as Snellen visual acuity, contrast sensitivity, or complex visual activities of daily living.

The authors have linked peripheral retinal damage produced by PRP with changes in the visual cortex. While questions remain, I encourage the authors to expand their observations.

REFERENCES

1. Parver, LM. Photochemical injury to the foveamacula of the monkey eye following argon blue-green panretinal photocoagulation. *Tr Am Ophth Soc* 2000;98:365-374.

[Editors note] DR THOMAS R. HEDGES JR. wondered about the occasional recovery of central and peripheral vision in some patients after brain lesions. He pointed out that in the macula the cone projections are magnified between the eye and the visual cortex and asked if the authors could use markers to quantify the changes in these pathways and perhaps explain the extraordinary plasticity of the brain for recovery.

DR T. MICHAEL NORK. Dr Parver correctly points out a limitation of our study, namely that there could have been subtle changes in the levels of these neurochemicals in the macular region of the visual cortex that were below the threshold of detection by the immunochemical and histochemical methods that were employed. Therefore, we cannot rule out the possibility that peripheral laser photocoagulation has an effect on this region of the cortex.

In response to Dr Thomas Hedges, Jr's suggestion that the central retinal pathways be further investigated by performing macular photocoagulation, we agree that an experiment such as this might be informative. We chose panretinal photocoagulation for this study because it is a commonly used treatment in humans to control retinal and iris neovascularization.